JOURNAL OF MATERIALS SCIENCE 37 (2002) 4197–4202

Simulation of creep crack growth in ceramic composites

P. SODANAPALLI, D. N. COON
Mechanical Engineering Department, University of Wyoming, Laramie, WY 82071, USA
E-mail: dcoon@uwyo.edu

The elevated temperature response resulting from tensile creep of fiber reinforced ceramic composites was modeled using Monte Carlo simulation. The model consisted of a uniaxially loaded fiber tow aligned with the direction of applied load, and modeled the growth of matrix cracks resulting from creep failure of bridging fibers. A creep strain rate consisting of primary and steady state components was assumed, and each component was modeled by a power law relationship. Power law creep exponents in the range of 2.0–2.5 for a selected SiC/SiC system at stress levels ranging from 60 MPa to 200 MPa were evaluated. Fatigue-like behavior was predicted as a result of tensile creep, and a fatigue exponent of 3.03 ± 0.07 was predicted for nominal stress levels less than 200 GPa. The influence of initial crack length on failure lifetime was also studied, but was found to have little influence on the predicted lifetime. The predicted failure response suggested a stress dependent creep process could be used to model experimental data and evaluate the failure mechanism of reinforced composites.

1. Introduction

Ceramic matrix composites (CMCs) are candidates for applications in which creep life elevated temperature is an important material characteristic. There is a need to understand and predict the creep deformation behavior of CMCs as a function of basic properties of the constituent phases. Such information is vital to identification and development of ceramic composites exhibiting improved creep and elevated temperature fatigue resistance.

Fatigue-like behavior of CMCs at high temperatures has been reported [1–8]. Several degradation mechanisms have been identified including creep, fiber/environment reaction, and wear of the fiber surfaces during cyclic loading. Although it suspected that multiple degradation mechanism may be simultaneously active in experimental studies, creep has been identified as the predominant damage mechanism resulting in fatigue-like behavior at elevated temperatures [7–12].

Characterizing the physical and mechanical properties of fibers and composite materials requires statistical and probabilistic concepts [13–16]. Monte Carlo simulation is the numerical solution of analytical models containing probabilistic characteristics. In Monte Carlo simulation, a computer calculates system behavior following well-defined mathematical relationships involving these probabilistic characteristics. The validity of the numerical solution is determined in part by the appropriateness of the mathematical relationships and in part by the values of the various probabilistic characteristics. While any single solution will depend on the specific values of the probabilistic characteristics, performing the numerical solution many times can give insight into the behavior of the physical system.

The purpose of this communication is to report predicted fatigue-like behavior resulting from tensile creep of a unidirectional SiC/SiC ceramic composite. The model described in this communication isolates creep from the other possible degradation mechanisms. The modeling approach was based on Monte Carlo simulation, creep of bridging fibers in a cracked composite, crack growth resulting from creep failure of bridging fibers, and eventual global failure of the composite.

2. Monte Carlo creep model

The Monte Carlo model described in this communication simulated quasi-static crack growth due to creep of fibers in a rectangular tow that was loaded externally in tension. The sequence of steps used to simulate the above system is described in the following sections.

2.1. Fiber tow

The material was assumed to be a rectangular fiber tow that consisted of uniformly spaced, unidirectional fibers impregnated in the matrix, and the fibers were arranged in 12 rows and 41 columns for a total of 492 fibers [13–15]. The fibers were aligned in the direction of an externally applied load as shown in Fig. 1.

Matrix cracking, typically originating from preexisting flaws, was included in the model as a single matrix crack with intact bridging fibers over its entire surface. The crack was oriented perpendicular to the applied stress as shown in Fig. 1. The initial length of the matrix crack could be selected during initialization of the model, and was typically set at 5% of the tow length.

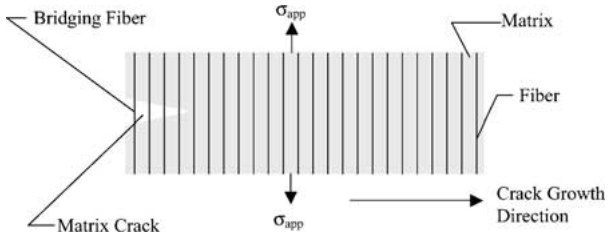

Figure 1 Schematic representation of composite modeled in this communication.

A crack length equivalent to 5% of the tow length would result in immediate failure of a monolithic material. However, bridging fibers in a composite material could stabilize such a crack under lower levels of applied stress. Crack stability in the model described in this communication was determined using the concepts of linear elastic fracture mechanics [17]. The applied stress intensity factor, K_{I}, was computed and compared with the critical stress intensity factor K_{IC} If K_{IC} was greater than K_{I}, the crack was stable. Otherwise the crack was extended to the next fiber column and checked for stability. This process of crack extension (i.e., crack growth) increased the number of bridging fibers by one entire column of fibers, and was repeated until crack stability was achieved.

2.2. Distribution of load within fiber tow

External load was distributed to the individual fibers using an isostrain assumption [13–15]. This approach assumed that the individual fibers and the matrix were in a state of uniform strain. The matrix that was in front of the crack tip was assumed to carry mechanical load that was of the same magnitude as the load carried by the fiber. This assumption was reasonable since both the matrix and the fiber modeled in this study were silicon carbide. The load acting behind the crack tip was carried entirely by the bridging fibers. The stress on the individual fibers ($\sigma_{i,j}$) behind the crack tip (i.e., bridging fibers) under isostrain conditions was calculated from [13]:

$$\sigma_{i,j} = \left(\frac{\sigma_{\mathrm{app}}}{V_f}\right)\left(\frac{E_{i,j}}{\bar{E}}\right) \tag{1}$$

where σ_{app} = applied stress, V_f = the fiber volume fraction, $\bar{E}$ = average modulus of fiber array, $E_{i,j}$ = modulus of the fiber i, j, i = horizontal position of fiber in the tow, j = vertical position of fiber in tow.

Since both fibers and the matrix were assumed to take the load in front of the crack tip, the stress on the fibers in front of the crack tip was taken as $\sigma_{\mathrm{applied}}$. In this manner, the bridging fibers were modeled as existing under higher states of stress than fibers in front of the crack tip.

The total force on all bridging fibers normalized to the surface area of the crack is given by [15]:

$$\sigma_b = \frac{a(\sigma_{\mathrm{crack}})}{S} \tag{2}$$

where σ_b = equivalent stress resulting from bridging fibers, S = surface area of the crack, a = total area of all individual fibers in the bridging zone, σ_{crack} = sum of stresses carried by the fibers behind the crack tip.

The applied stress intensity factor, K_{I}, for the composite was calculated by [15]:

$$K_{\mathrm{I}} = Y(\sigma_{\mathrm{app}} - \sigma_b)\sqrt{C\pi} \tag{3}$$

where C = the crack length, Y = a constant ($\pi^{1/2}$ for an edge loaded surface crack).

Using Equation 3, the existence of bridging fibers effectively reduced the influence of applied loads [17]. Equation 3 was used to compare to the applied stress intensity to the fracture toughness to assess the mechanical stability of the crack.

3. Creep strain rate model

The total creep rate, $\dot{\varepsilon}_{\mathrm{tot}}$, was expressed as the sum of the primary creep rate, $\dot{\varepsilon}_p$, and the steady state creep rate,$\dot{\varepsilon}_s$, according to [18]:

$$\dot{\epsilon}_{\mathrm{tot}} = \dot{\epsilon}_p + \dot{\epsilon}_s \tag{4}$$

Primary creep was determined from [18]:

$$\dot{\varepsilon}_p = A\sigma^p t^m \tag{5}$$

where A = stress independent constant, σ = stress, t = the time elapsed since the loading, p = stress exponent for primary creep, m = time exponent for primary creep.

Negative values of m would correspond to a decreasing primary creep rate with time.

Steady state creep strain rate was modeled as a power law [19]:

$$\varepsilon_s = B\sigma^{n_{\mathrm{ss}}} \tag{6}$$

where σ = stress, n_{ss} = stress exponent for steady-state creep, B = a constant.

The physical effect of creep was modeled using a constant volume assumption, and this assumption resulted in a reduction in fiber cross-sectional area as a consequence of creep according to [13]:

$$A_{i,j}^{\mathrm{new}} = \frac{A_{i,j}^{\mathrm{prev}}}{\varepsilon_{\mathrm{tow}} + 1} \tag{7}$$

where $A_{i,j}^{\mathrm{new}}$ = cross sectional area of fiber i, j after creep, $A_{i,j}^{\mathrm{prev}}$ = cross sectional area of fiber i, j prior to creep.

The stress in the individual fibers after creep was then calculated from:

$$\sigma_{i,j}^{\mathrm{new}} = \frac{F_{i,j}}{A_{i,j}^{\mathrm{new}}} \tag{8}$$

where $\sigma_{i,j}^{\mathrm{prev}}$ = stress in fiber i, j after creep, $F_{i,j}$ = force acting on fiber i, j.

The combination of Equations 7 and 8 resulted in an increase in stress for all fibers undergoing creep. Each iteration of the simulation in which the fibers were allowed to creep was known as a timestep. The reduction of fiber radius in each timestep resulted in increased stress on the fiber under a constant load.

TABLE I Monte Carlo variables of fiber characteristics [13–15] used in this study. SD signifies the standard deviation

Fiber characteristic	Distribution type	Value		
		Mean	SD	Weibull modulus
Radius	Gaussian	6.9 υm	1.3 υm	
Strength	Weibull	1.1 GPa		3.6
Modulus	Gaussian	145 GPa	30 GPa	

TABLE II Standard mechanical parameters [13–15] used in the numerical simulation

Parameter	Value
Initial crack length (a_o)	5% of tow length
Stress intensity factor (K_I)	4.0 MPa $\cdot$ m$^{1/2}$
Applied stress (σ_{app})	110 MPa
Fiber volume (V_f)	40%
Array size of the fibers (i X j)	12×41
Stress exponent (n_{ss})	2

The stress on the fiber increased until the fiber stress reached the fiber strength. At this point the fiber broke, and the load on the broken fiber was distributed to unbroken fibers using an inverse square law previously reported [13–15]. Following load redistribution, crack stability was checked, the matrix crack was allowed to grow as appropriate, creep was applied to individual fibers, and fibers stresses were again compared to fiber strengths. In this way the Monte Carlo simulation was iterated until complete failure all fibers in the tow occurred.

The details of the numerical approach have been previously reported [13–15]. The parameters and the statistical distributions used in the Monte Carlo model described in this communication are given in the Table I. Chi-Square and Kolmogorov-Smirnov statistical tests were used to verify the randomness and compatibility of parameter distributions generated [13–15]. The standard mechanical properties of the composite are given in Table II, and these values were used as default values unless other values were selected during initialization of the model.

4. Results

Pure mechanical failure of a small number of fibers was predicted on initial application of stress. This mechanical failure occurred in weaker fibers generated from the strength distribution, and was consistent with previous numerical studies [13–15, 20]. The simulation allowed all fibers to creep under load. The fibers in front of the crack carried smaller loads than the bridging fibers since a portion of the load in front of the crack was carried by the matrix phase. Accumulation of creep strain led to the failure of some bridging fibers, which led to the weakening of the bridging zone. This weakening of the bridging zone led to crack growth until the crack stabilized by formation of additional bridging fibers. This process was continued until all the fibers were broken.

There were three distinct regions in the simulated failure of a fiber tow resulting from creep failure of bridging fibers: crack growth incubation, crack growth,

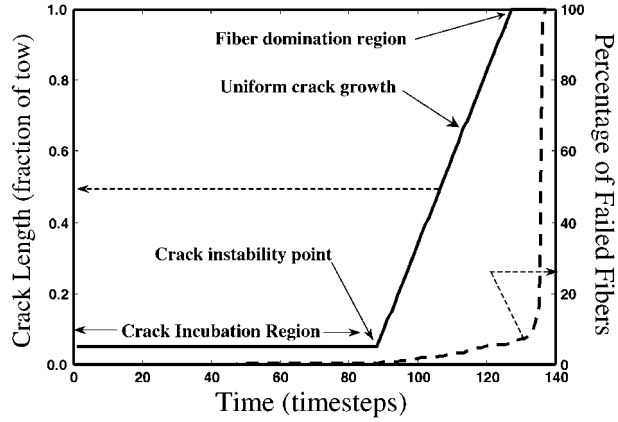

Figure 2 Predicted crack length (as a fraction of tow length) and percentage of failed fibers as a function of time. The input parameters used were those given in Tables I and II with the exception of applied stress which was 85 MPa.

and fiber domination. The three distinct regions of behavior are shown in Fig. 2. Crack growth incubation was an initial period where small numbers of failed bridging fibers resulted in crack stability in the absence of the formation of new bridging fibers by crack growth. The crack growth incubation region was followed by the crack growth phase in which the crack propagated through the matrix at a fairly constant rate giving way to the fiber domination phase. Fiber domination was characterized by complete matrix cracking and a short period of rapid fiber failure leading to failure of the composite. The most interesting characteristics illustrated in Fig. 2 are the length of the crack incubation region, the instability point (iteration step where the crack became unstable), crack propagation rate, fiber domination point (iteration step where the complete matrix was cracked and fibers dominated the system), and lifetime. Each of the above characteristics was studied by systematically varying the standard mechanical parameters given in Table II.

The total number of timesteps indicates the total number of numerical creep steps completed for the failure of the whole fiber tow. In this way the number of timesteps to failure gives a relative measure of the predicted lifetime of the fiber tow. As shown in Fig. 2, the total number of timesteps required for complete failure of the fiber tow was 137. There was complete fiber domination beginning at timestep 126. It is apparaent from Fig. 2 that 90% of fibers broke in the last 10% of lifetime, and this prediction agrees well with published data [2–7].

Since the primary objective of a Monte Carlo simulation is to extract information about typical system behavior, the average response of several individual solutions is typically computed. One concern is the number of individual solutions necessary to generate a meaningful average. The convergence analysis of the Monte Carlo simulation described in this communication for up to 100 independent solutions of the simulation is shown in Fig. 3. This convergence analysis showed that the simulation yielded identical values of the mean and standard deviation when the number of individual solutions in each data set was above 35. Therefore, 50 independent simulations were conducted for each variation of a mechanical parameter in the current study.

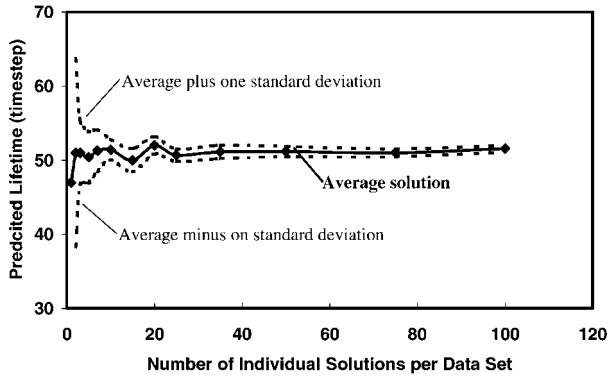

Figure 3 Convergence analysis of the Monte Carlo simulation described in this communication. The input parameters were held constant at the standard values (Tables I and II).

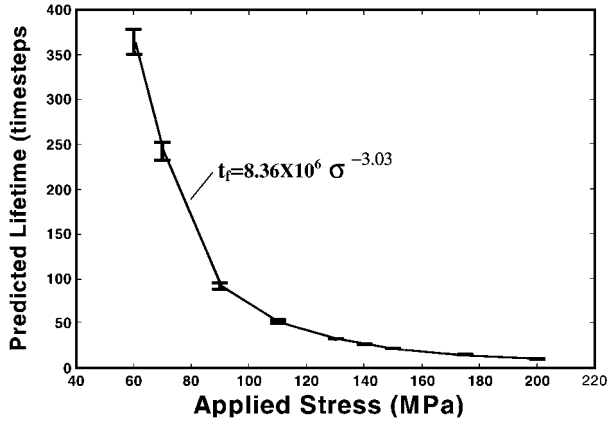

Figure 4 Predicted lifetime as a function of applied stress from 60 to 200 MPa. There are 50 individual solutions in each data set. The error bars are ± one standard deviation.

4.1. Effect of applied stress

The primary motive for the simulation described in this communication was to model the effects of applied stress on the creep life of the fiber tow. The simulation was used to model the effect of applied stress levels ranging from 60 MPa to 200 MPa. The average predicted lifetime for 50 independent simulation solutions as a function of applied stress is shown in Fig. 4. The plot clearly shows that the predicted lifetime of the fiber tow decreased nonlinearly as the applied stress increased. In addition, the standard deviation of the 50 individual solutions, shown as error bars in Fig. 4, decreased as the applied stress increased.

Fatigue-type behavior is characterized as the nonlinear decrease with lifetime with increased applied stress, and is traditionally modeled with the following expression [13]:

$$t_f = A(\sigma_{\text{app}})^{-n_f} \tag{9}$$

where t_f = lifetime, A = constant, n_f = fatigue exponent.

Shown in Fig. 4 is the best-fit curve for the predicted lifetime as a function of applied stress using the standard form given Equation 9. The fatigue exponent and 95% confidence bound was computed to be 3.03 ± 0.07. This fatigue exponent predicted from the model described in this communication compares very well to the reported value of 2.92 ± 0.04 for this composite material [4, 5].

It was observed that there was no predicted crack propagation even in the absence of bridging fibers if the applied stress was less than 68.5 MPa. This lack of crack propagation was due to the critical effective stress that resulted in crack instability in the absence of bridging fibers as given by:

$$\sigma_{\text{critical}} = \frac{K_{\text{IC}}}{Y\sqrt{\pi C}} \tag{10}$$

where σ_{critical} = critical effective stress for crack unstable, K_{IC} = fracture toughness of the composite, C = initial matrix crack length.

From Equation 10, it can be concluded that if the applied stress is below the critical effective critical stress, then there will not be any crack growth in the composite. If all the bridging fibers were assumed to be intact, then the critical applied stress to cause the crack growth (at a crack length of 5% of the tow length) was approximately 82.9 MPa. The above results are in agreement with the possibility of an infinite lifetime for low stresses (fatigue limit), and are consistent with previous numerical studies [15].

4.2. Effect of initial crack length

The influence of the initial matrix crack length and its effect on the predicted lifetime of the fiber tow was examined. A set of simulations was completed in which the initial matrix crack length was systematically varied from 2.5% of tow length to 100% of tow length (fully cracked matrix). Fig. 5 shows the relationship between initial matrix crack length and lifetime. Fig. 5 shows that there is little functional dependence of initial matrix crack length on lifetime beyond an initial matrix crack length 5% of tow length. This observation suggests that the lifetime of the fiber tow depended largely on the fiber behavior during the fiber-dominated region rather than on the initial matrix crack length for the standard mechanical parameters, Table II.

The initial matrix crack length was not stable for lengths from 2.5% to 5% of the fiber tow length for an applied stress of 110 MPa. The crack propagated to a longer length under applied stress irrespective of its initial length. This observation can be explained using the following fracture mechanics relation [21]:

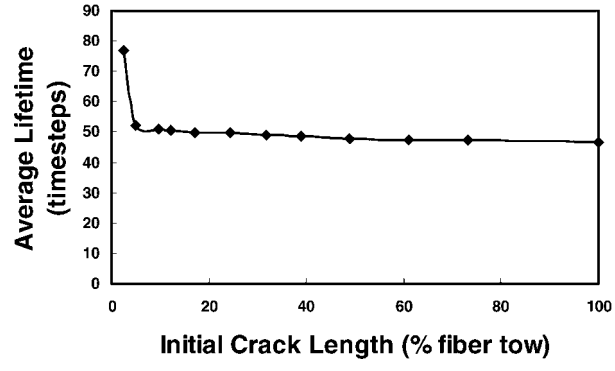

Figure 5 Effect of initial crack length on the predicted lifetime. The data points are averages of 50 individual solutions, and the one standard deviation error bars were smaller than the height of the data points. All input parameters were held constant at the standard values (Tables I and II) except for initial crack length.

$$C_{\text{critical}} = \frac{1}{\pi}\left[\frac{K_{\text{IC}}}{Y(\sigma_{\text{app}} - \sigma_b)}\right]^2 \qquad (11)$$

where C_{critical} = critical crack length below which crack is unstable, K_{IC} = fracture toughness of the composite. From Equation 11, it may be observed that there is a critical crack length below which the crack is unstable for a given level of applied stress. At a matrix crack length greater than the critical value, the increased number of bridging fibers and corresponding increase of the effective stress resulting from the bridging fibers, σ_b, provided crack stability. The instability of matrix crack lengths less than the critical value led to crack growth until the crack attained stability by increased numbers of bridging fibers. However, an extremely short initial matrix crack length would be inherently stable for lower applied stress levels, Equation 10, and would lead to increased creep lifetime due to an extensive crack growth incubation region, Fig. 2.

4.3. Effect of steady-state creep stress exponent

The steady-state creep strain rate was modeled using a power law, Equation 6. The influence of the steady-state creep stress exponent (n_{ss}) on the predicted lifetime of the fiber tow was studied. The stress exponent was varied from 2 to 2.5 and the results are plotted in Fig. 6. It is apparent in Fig. 5 that the predicted lifetime was very sensitive to the changes in the steady-state creep stress exponent. For steady-state creep stress exponent values that are greater than 2.25, the predicted failure of all the fibers in the tow occurred in only one or two timesteps for an applied stress of 110 MPa (10% of the average fiber strength) and an initial matrix crack length of 5% of the tow length. It was also observed that the matrix was not fully cracked in the above cases, and the fiber bridging mechanism seem to have been dominated by the creep of the fibers.

Steady-state creep stress exponents as high as 6 have been reported for SiC/SiC composite systems [1–3], and these systems exhibited appreciable creep lifetime. The short creep lifetime predicted for steady-state creep stress exponents in excess of 2.25 (Fig. 6) does not conflict with these experimental results. The creep lifetime is determined by the cumulative influences of steady-state creep stress exponent, applied stress, fiber strength, and initial matrix crack length. The model parameters used to predict the behavior shown in Fig. 6 included high values of applied stress (10% of the fiber strength) and a relatively large initial matrix crack length (5% of the tow length). It is quite reasonable to expect appreciable creep lifetime with a steady-state creep stress exponent as high as 6 for composites under lower applied stresses and/or much smaller initial crack lengths. However, the general trend evident in Fig. 6 of a nonlinear decrease in creep lifetime with increased steady-state creep stress exponent is still predicted for other values of applied stress and initial matrix crack length.

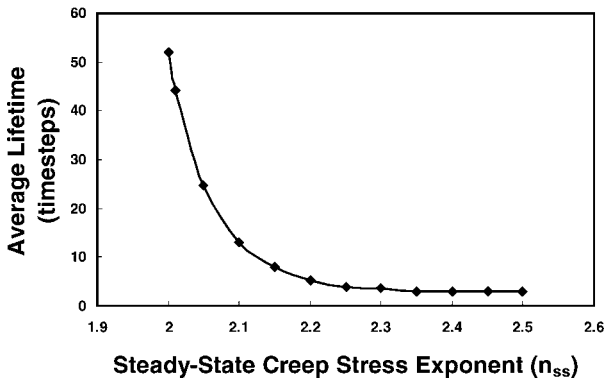

Figure 6 Influence of the steady-state creep stress exponent on the predicted lifetime. All input characteristics except the steady-state creep stress exponent were held constant at the standard values (Tables I and II). The data points of averages of 50 individual solutions, and the one standard deviation error bars are smaller than the data points.

5. Conclusions

Tensile creep behavior and elevated temperature fatigue of fiber reinforced ceramic composites were investigated using a Monte Carlo model. The model consisted of a uniaxially loaded fiber tow composed of unidirectional fibers aligned in the direction of the load. The model described in this communication specifically addressed creep degradation of fibers bridging relatively large matrix cracks. Relatively large matrix cracks are known to be mechanically stable in the presence of bridging fibers. The degradation of these bridging fibers was modeled as a time-dependent failure of bridging fibers, and the corresponding mechanical instability of the matrix crack. The model permitted an increase in bridging fibers as a result of growth of the matrix crack. In this manner, quasi-static crack growth was modeled as periods of crack stability and bridging fiber degradation followed by crack growth and formation of new bridging fibers.

The Monte Carlo variables were the fiber radius, elastic modulus, and strength. Both fiber and matrix phases were modeled as exhibiting creep, and the result of creep was modeled as increased stress in each phase. The model assumed a steady-state creep strain rate, which was approximated by a power law relationship. Applied stress was distributed through the composite using an isostrain assumption. The failure stress was used as the critical stress predicting failure. The creep lifetime corresponded to failure of all fibers.

The effects of steady-state creep stress exponents in the range of 2–2.5 for a selected SiC/SiC system at stress levels ranging from 60 MPa to 200 MPa were examined. Incubation of matrix crack growth, crack growth, and a region of fiber domination were predicted to precede final composite failure. It was predicted that the majority of fiber damage occurred very late in the creep lifetime with 90% of the fibers failing in the last 10% of the creep lifetime.

It was predicted that the creep lifetime of the composite was quite sensitive to the changes in the steady-state creep stress exponents. The initial crack length was predicted to have no effect on the creep lifetime for relatively large matrix cracks. Fatigue-like behavior, a nonlinear decrease in creep lifetime with increased applied stress, was predicted. A fatigue exponent of 3.03 ± 0.07 was predicted for nominal stress levels less than 200 GPa.

References

1. P. REYNAUD, D. ROUBY, G. FANTOZZI, F. ABBE and P. PERES, *Ceramic Transactions* **57** (1995) 95.
2. L. P. ZAWADA, L. M. BUTKUS and G. A. HARTMAN, *J. Amer. Ceram. Soc.* **74**(11) (1991) 2858.
3. S. RAGHURAMAN, J. F. STUBBINS, M. K. FERBER and A. A. WERESZCZAK, *Journal of Nuclear Materials* **212/215**(9) (1994) 840.
4. M. H. HEADINGER, P. GRAY and D. H. ROACH, Presented at the Composites and Advanced Structures Cocoa Beach Conference, January 1995.
5. M. J. VERILLI, A. M. CALAMINO and D. N. BREWER, presented at the Composites and Advanced Structures Cocoa Beach Conference, January 1995.
6. H. T. LIN, P. F. BECHER, K. L. MORE, P. F. TROTORELLI and E. LARA-CURZIO, Oak Ridge National Laboratory, 1996.
7. E. Y. SUN, S. T. LIN and J. J. BRENNAN, *J. Amer. Ceram. Soc.* **80**(3) (1996) 3065.
8. J. W. HOLMES, *J. Mater. Sci.* **26** (1991) 1808.
9. D. B. MARSHALL and B. N. COX, *Acta Metallurgica* **35**(11) (1987) 2607.
10. M. R. BEGLEY, A. G. EVANS and R. M. MCMEEKING, *Journal of the Mechanics and Physics of Solids* **43**(5) (1995) 727.
11. F. E. HEREDIOA, J. C. MCNULTY, F. W. ZOK and A. G. EVANS, *J. Amer. Ceram. Soc.* **78**(8) (1995) 2097.
12. J. A. DICARLO, *J. Mater. Sci.* **21**(1) (1986) 217.
13. D. N. COON and A. M. CALOMINO, *ibid.* **36** (2001) 2597.
14. F. MACDONALD and D. N. A. M. COON, *ibid.* **36** (2001) 1681.
15. D. N. COON and A. MOTKUR, *ibid.* **35** (2000) 3207.
16. D. H. WAGNER, "Application of Fracture Mechanics to Composite Materials," Vol. 6 (Elsevier Science Publishing Company, 1989) p. 39.
17. D. B. MARSHALL and A. G. EVANS, "Fracture Mechanics of Ceramics," Vol. 7 (1986) p. 1.
18. Y. H. PARK and J. W. HOLMES, *J. Mater. Sci.* **27** (1992) 6341.
19. S. R. CHOI, J. A. SALEM and N. N. NEMETH, *ibid.* **33**(5) (1998) 1325.
20. D. N. COON, *J. Materials Science and Technology* **9**(2) (2001) 65.
21. R. W. HERTZBERG, "Deformation and Fracture Mechanics of Engineering Materials" (John Wiley & Sons, 1989).

Received 20 July 2001
and accepted 21 May 2002